Cent. Eur. J. Phys. • 8(2) • 2010 • 169-177
DOI: 10.2478/s11534-009-0031-y

VERSITA

Central European Journal of **Physics**

Point-by-point inscription of 250-nm-period structure in bulk fused silica by tightly-focused femtosecond UV pulses: experiment and numerical modeling

Research Article

David N. Nikogosyan[1][2]*, Mykhaylo Dubov[1], Holger Schmitz[1], Vladimir Mezentsev[1], Ian Bennion[1], Padraig Bolger[3], Anatoly V. Zayats[3]

1 Photonics Research Group, Aston University, Birmingham B4 7ET, United Kingdom

2 Physics Department, University College Cork, Cork, Ireland

3 Centre for Nanostructure Media, IRCEP, The Queen's University of Belfast, Belfast BT7 1NN, United Kingdom

Received 10 December 2008; accepted 1 March 2009

Abstract: By conducting point-by-point inscription in a continuously moving slab of a pure fused silica at the optimal depth (170 µm depth below the surface), we have fabricated a 250-nm-period nanostructure with 30 nJ, 300 fs, 1 kHz pulses from frequency-tripled Ti:sapphire laser. This is the smallest value for the inscribed period yet reported, and has been achieved with radical improvement in the quality of the inscribed nanostructures in comparison with previous reports. The performed numerical modeling confirms the obtained experimental results.

PACS (2008): 42.79.Dj; 42.81.-i; 81.07.-b; 81.16.-c

Keywords: femtosecond UV laser • microfabrication • fused silica • nanostructure

1. Introduction

In 2004, two groups independently reported the application of a point-by-point (PbP) technique to fibre Bragg grating (FBG) inscription in standard non-photosensitive fibers [1–3]. Both groups used tightly-focussed femtosecond (fs) IR laser (λ = 800 nm) radiation and a submicron precision positioning system. The FBGs produced exhibited either fourth-order (Λ = 2.14 µm) [1] or from first- to fourth-order (with the strongest second-order, Λ = 1.07 µm) [2, 3] periods for the reflection peak at the telecommunications wavelength 1.55 µm. Since that time, the PbP technique employing the output of a femtosecond Ti:sapphire laser has evolved to become a relatively routine method for the fabrication of gratings in fibers with typical values of the inscribed period of 1.07 µm [3–8] or 1.12 µm (third-order grating for the 1080 nm reflection) [9]. Recently, with tightly-focused 800 nm femtosecond light pulses, injected into a slab of pure fused silica using a special, reflective microobjective, the fabrication of first-order gratings for 1550 nm wavelength (Λ = 0.535 µm) was reported [10, 11]. Very recently, by introducing index-

---

*E-mail: niko@phys.ucc.ie

matching fluid between the planar microscope cover slip and fiber, the same 535 nm period was achieved with FBG recording in standard fiber [12].

It should be noted that all of the foregoing investigations on point-by-point microfabrication have employed 800 nm femtosecond light pulses, which excite the samples of fused silica (or germanosilicate glass) via five-photon absorption [13]. Such a multi-photon approach can employ the different wavelengths and different numbers of photons in one elementary absorbing act [14], so facilitating inscription inside various non-photosensitive optical materials. It is also known that the propagation of a femtosecond 800 nm pulse inside a bulk dielectric (e.g. fused silica glass) with a peak power exceeding the threshold (critical power) results in self-focusing. Remarkably, this regime is characterized by reduction of the spatial dimensions of the photoinduced material modifications below the diffraction limit [15]. Since the achieved size of the pitch (modification) is about 270 nm and much smaller than the inscribing wavelength of 800 nm, further feature size reduction would appear to be highly unlikely using this method. However, shifting the wavelength of the inscribing Ti:sapphire laser radiation into the UV range (e.g. to 267 nm with simultaneous decrease in the order of absorption process from five-photon to two-photon [14]) immediately makes it possible to record structures with even smaller periods. Such a development is very important, for example, for the point-by-point fabrication of first-order Bragg gratings possessing a peak reflectance wavelength of ~1 µm.

In our previous work, the use of 267 nm femtosecond pulses with 82 nJ energies led us to the inscription of 300-nm-period structures [16]. In the current work, the optimising of the inscription depth has allowed us to decrease the inscription energy down to 30 nJ and to inscribe the 250-nm-period structure. The quality of the nanostructures was significantly improved in comparison with previous report. Besides, in current work we provide the theoretical estimations for major physical parameters involved in two-photon UV inscription as well as the preliminary results of numerical simulations.

2. Experimental set-up

Femtosecond pulses at 800 nm were produced by a Ti:sapphire chirped pulse amplification laser system consisting of a„Tsunami“ oscillator and a „Spitfire“ amplifier (both from Spectra-Physics). The laser system delivered 0.8 mJ pulses with 150 fs duration and 1 kHz repetition rate. The IR beam diameter after the amplifier was 2.5 mm at FWHM. The set-up for third-harmonic generation (THG) was similar to that described earlier [17]. The pulses at 267 nm were produced by non-collinear sum-frequency mixing between fundamental radiation and that at the second harmonic (Fig. 1a). A half-wave plate was used to distribute the energy of 800 nm pulses between two channels, which allowed us to manipulate the energy at the entrance of second-harmonic generator and, thus, the energy of the output radiation at 267 nm. The pulses at 400 nm were produced in a 1 mm thick BBO crystal cut for type I collinear second harmonic generation ($\theta = 29.2°$, $\phi = 90°$) [18]. A second half-wave plate was used for 90° polarization rotation of the 400 nm beam. Using three mirrors with high reflectance at 400 nm, the second harmonic beam was separated from the fundamental. The 400 and 800 nm pulses were directed into a 1.0 mm thick BBO crystal cut for type I sum-frequency generation ($\theta = 44.3°$, $\phi = 90°$) [18]. The angle between the 800 nm and 400 nm beams was less than 2° in the horizontal plane. Using highly-reflecting UV mirrors and the non-collinear geometry of THG, we easily separated the 267 nm radiation. The UV pulse energy was monitored by a PD10 photodiode (Ophir Optronics). The energy of the third harmonic pulses was about 80 µJ with pump energy at 800 nm of 800 µJ. By varying the optical delay and measuring the cross-correlation function between the fundamental pulse and it's second harmonic, we estimated the width of both 400 nm and 267 nm pulses to be about 300 fs.

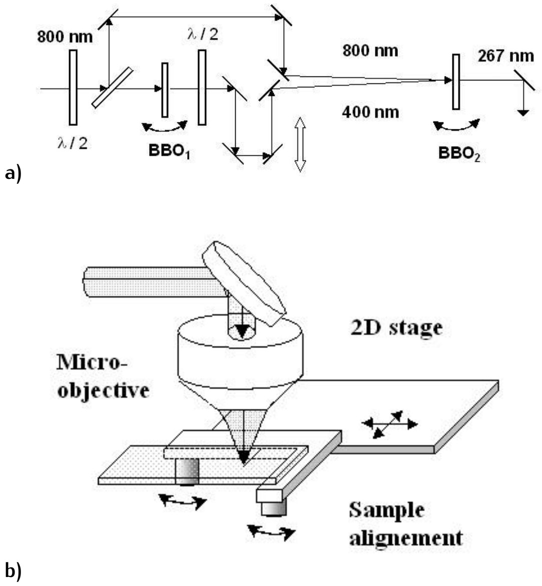

Figure 1. (a) Experimental set-up for third-harmonic generation; (b) PbP inscription set-up.

Fused silica samples of 50×20 mm size and 1 mm thickness (Schott Glas) were used in the experiments. They were moved in the horizontal plane in two perpendicular directions by an air-bearing translation stage ABL-1000 (Aerotech). The translation speed was varied in the range of 0.2-5.0 mm/s. The absolute and relative micropositioning accuracies were both better than 50 nm.

The UV laser beam was directed in a strictly perpendicular direction on to the surface of the fused silica sample from the top (Fig. 1b). It could be focused to any selected depth between 0 and 600 μm below the surface with accuracy of 1 μm. For focusing, we used a reflective microscope objective with numerical aperture of 0.65 (Ealing), manipulated by a 3D-micropositioning manual translation stage 17 MAX 303 (Melles Griot). The inscription energy values were varied between 20 and 400 nJ, whilst the length of inscribed tracks was usually between 0.5 and 4 cm.

3. Characterisation of inscribed structures

To establish the optimal conditions for inscription, one should carefully adjust at least four parameters including, particularly, the laser pulse energy, the speed of translation stage movement, the focus depth inside the sample, and the polarization of the inscribing light with respect to the direction of sample movement. Other parameters, including the numerical aperture of the microscope objective, the repetition rate, the wavelength and the duration of the inscribing pulses, also could be varied. The resulting number of experimental tracks could easily reach some thousands: thus, an express visualization method is needed for such optimisation.

We perform the characterisation of the irradiated samples using an optical microscope, Axioscope-2 MOT plus (Zeiss), which was equipped for both transmitted light and differential interference contrast (DIC) measurements. The resolution of a conventional optical microscope is considered to be of the order of the illumination wavelength: in our experiment, even with the use of a blue filter it was rather difficult to distinguish the 400-nm-period perturbations induced in the bulk of the material. However, the use of DIC technique enabled us to monitor structures with periods down to 250 nm. In the experiments, we used the combination of a Plan-Apochromat oil immersed objective (×100/1.40/DIC) and an Achromatic-Aplanatic condenser (1.4H/PH/DIC) with numerical aperture of 0.6 (or higher). A DIC-prism (III/1.4) and DIC-slider (×100/1.40III) were also used; such a combination seems to be the best one commercially available from Zeiss. The refractive index variation is expected to be of the order of 10^{-4}, which corresponds to a few times more than the sensitivity level of this DIC microscope, based on the comparable experiments conducted with known samples.

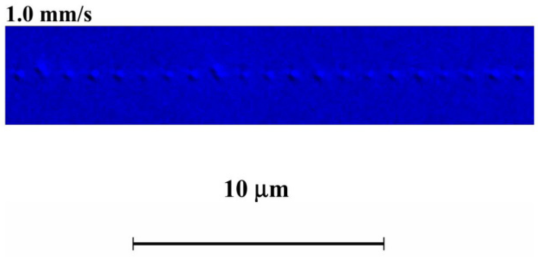

Figure 2. DIC microphotograph of the 1000-nm-period nanostructure, fabricated on the surface of a fused silica sample. The energy of the inscribing pulses was 38 nJ. The size of the bar corresponds to 10 μm.

It is important to note that DIC microscopy does not present the real image; rather, the resulting picture contains the information of both the intensity distribution and the derivative of the optical phase between two orthogonally polarised beams, spatially separated by a distance *smaller* than the resolution of the ×100, NA = 1.4 microscope objective. Thus, periods of about few hundred nanometres can be detected.

For the independent resolution check of DIC microscopy, some tracks exhibiting topographic changes of the sample surface were characterized with atomic-force microscopy (AFM) [19]. We used a commercial instrument, the Dimension Nanoscope III (VEECO), working in the tapping mode.

4. Results and discussion

We allied the optimisation procedure to the search for the optimal focus depth whereby inscription with smaller energy (leading to smaller beam diameter and, hence, to smaller nanostructure period) will be possible. In contrast with [16], in this work we used only the π polarization of the 267 nm inscribing beam (parallel to the translation direction).

We started our inscription experiments by focussing our microscope objective on the surface of the fused silica sample. With pulse energy as small as 38 nJ, we were able to record nanostructures with a translation speed of 1.0 mm/s. Taking into account the repetition rate of 1 kHz, it is easy to deduce that the recorded grating nanostructure possesses a 1000 nm period (Fig. 2). The DIC microphotography taken at the surface of our fused silica sample shows that the laser beam cross-section in the focal plane is not ideal and varies in size from pulse to pulse. A similar picture was revealed by topographic changes of the sample surface while using the AFM technique (Fig. 3a). The asymmetry seen in individual voxels is probably related to the light diffraction on wire holders of a small mirror inside the microobjective. From further consideration it will be evident that such diffraction becomes unimportant while focussing inside the slab of fused silica. We have also applied the AFM method for the independent calibration of our DIC microscopy approach. Fig. 3b (cross-section of the image of Fig. 3a along the grating) shows that 10 periods of our nanostructure inscribed on the surface of fused silica sample correspond exactly to 10 μm length, confirming our calibration shown at Fig. 2 (the scale bar is 10 μm). The cross-section in the perpendicular direction (presented in Fig. 3c), which is an ablation profile, gives an upper estimate of 400 nm for the diameter of the laser beam cross-section at FWHM at the surface of our sample, which agrees with the spot sizes deduced from Fig. 2 (210—310 nm).

To estimate the beam-waist diameter in the focal plane, one can use the well-known expression for diffraction-limited focusing, $w_0 = C\lambda/NA$, where λ is the inscription wavelength, C is a constant ~1.2-1.6, defined by the exact profile of the laser beam, and NA is the numerical aperture of the microscope objective. Substituting $\lambda = 267$ nm and $NA = 0.65$ gives the beam-waist diameter w_0 of 500-600 nm, which agrees with the experimental values given above.

Much better results - inscription at smaller translation speed values down to 0.25 mm/s - were obtained with the inscribing light tightly focussed to a depth of 170 μm below the surface of a fused silica sample. Fig. 4a demonstrates the periodic structures obtained using 30 nJ pulses with sample translation speed values of 1.0, 0.5, and 0.4 mm/s, respectively, *i.e.* with periods 1000, 500 and 400 nm, respectively. The excellent quality of the gratings obtained should be emphasized (*cf.* structures with similar periods obtained in our previous work [16] and depicted in Fig. 4b). Furthermore, the irregularity in spot size was strongly reduced.

The measurements of the diameter of the spots presented in Fig. 4a show that the decrease of the translation speed value from 1.0 mm/s to 0.5 mm/s and further to 0.4 mm/s leads to the simultaneous decrease of the single-pitch diameter from 630 nm to 300 nm and then to 230 nm (with accuracy ± 10 %). Interestingly, a similar feature could be seen in the tracks with similar periods presented in our previous report (Fig. 4b). This could be related to the change in glass properties (e.g., induced UV absorption and/or refractive index change) performed by the previous inscription pulse (pulses), which increases the absorption and hence following self-focusing for the next inscription pulse (pulses). The decrease of the translation speed value should increase the probability of such effect.

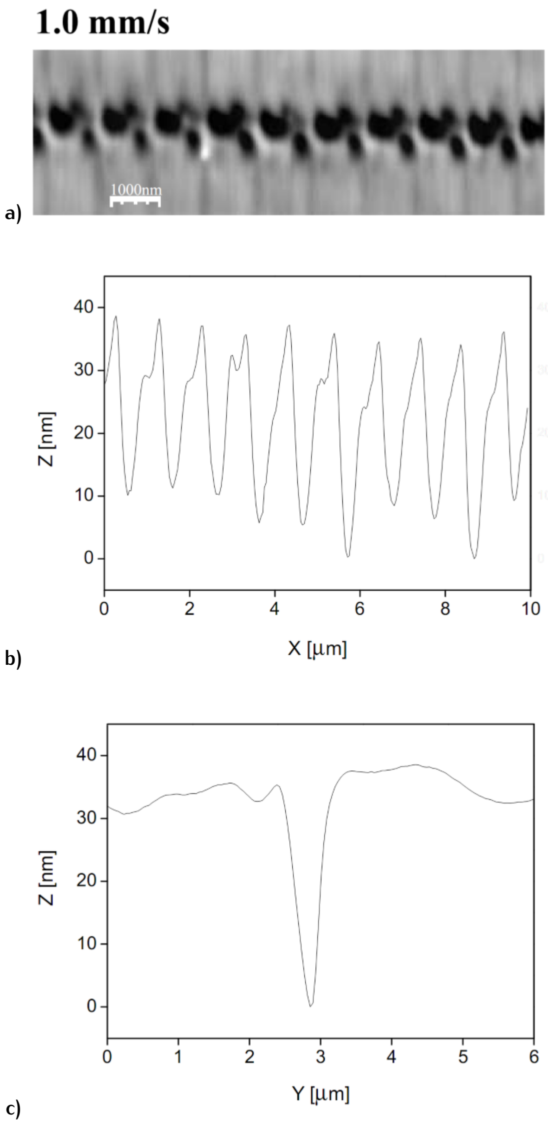

Figure 3. (a) Topography of the same 1000-nm-period nanostructure as in Fig. 2, investigated by AFM; (b) Cross-section of the image, presented in Fig. 3 a, along the inscription direction. (c) Cross-section of the image, presented in Fig. 3a, perpendicular to the inscription direction.

Fig. 5 shows the nanostructures obtained at the same focus depth (170 μm) using sample translation speed values 0.3 and 0.25 mm/s, *i.e.* with periods of 300 and 250 nm, respectively. The deterioration of quality of these gratings could be connected with overlapping between neighbouring spots (if the size of a spot exceeds a half of the nanostructure period, *i.e.*, 150 nm) and/or with the nanostructure period smaller than the resolution limit of DIC microscopy. Future investigation of recorded structures by

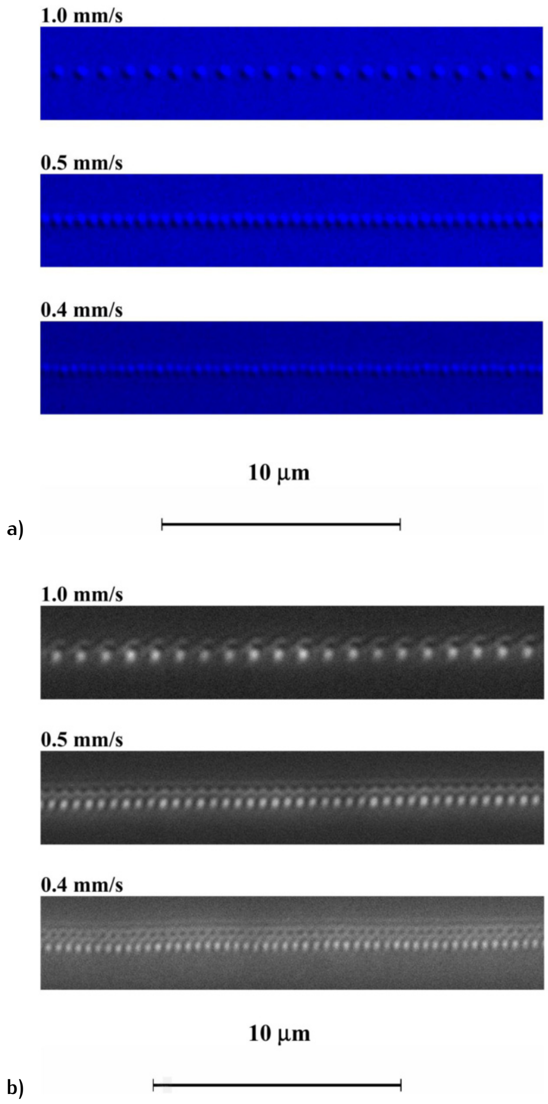

Figure 4. (a) DIC microphotographs of structures with 1000, 500 and 400 nm periods inscribed at the optimal focusing depth of 170 µm with sample translation speeds of 1.0, 0.5 and 0.4 mm/s, respectively. The energy of the inscribing pulses was 30 nJ. The size of the bar corresponds to 10 µm. (b) DIC microphotographs of similar structures inscribed earlier at a focus depth of 300 µm [16]. The energy of the inscribing pulses was 82 nJ. The size of the bar corresponds to 10 µm.

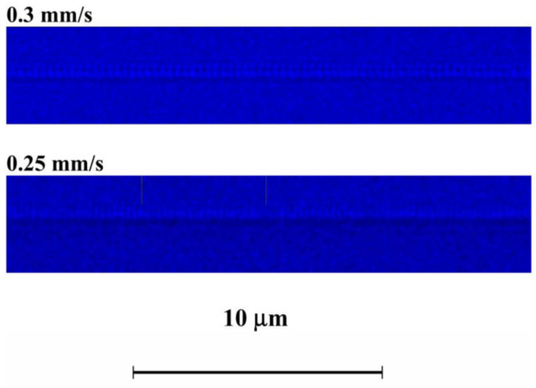

Figure 5. DIC microphotographs of structures with 300 and 250 nm periods inscribed at the optimal focus depth of 170 µm with sample translation speeds of 0.3 and 0.25 mm/s, respectively. The energy of the inscribing pulses was 30 nJ. The size of the bar corresponds to 10 µm.

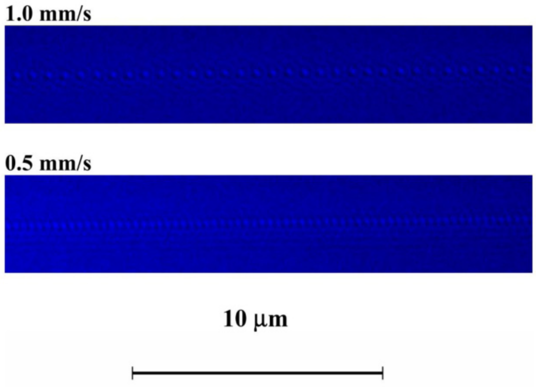

Figure 6. DIC microphotographs of structures with 1000 and 500 nm periods inscribed at a focus depth of 330 µm with sample translation speeds of 1.0 and 0.5 mm/s, respectively. The energy of the inscribing pulses was 90 nJ. The size of the bar corresponds to 10 µm.

scanning electron microscopy would help to elucidate this point. In any case, in this work at optimal focus depth, we have obtained evidence for nanostructure inscription with a period as small as 250 nm. We recall that, in our previous report [16], for this particular polarization of the inscribing laser beam only the 400-nm-period structure was recorded.

The importance of using the optimal focus depth can be illustrated by experiments conducted at 330 µm below the sample surface. At this focus depth, using 89 nJ pulses, we managed to record structures with periods down to 500 nm (Fig. 6); at the optimal inscription depth (170 µm), with 92 nJ pulses, we recorded the structures of 400- and 300-nm periods (Fig. 7).

It should be noted that the value of the optimal inscription depth obtained in this work (170 µm), differs from the one obtained in our previous report (300 µm). The reason for this could be the inaccurate positioning of the correction ring of the reflective microscope objective. Due to this, in our previous work, the reflective microscope objective was not aligned for minimisation of aberrations whilst being focussed on the surface of the sample (as was done in this investigation). It is necessary to underline that

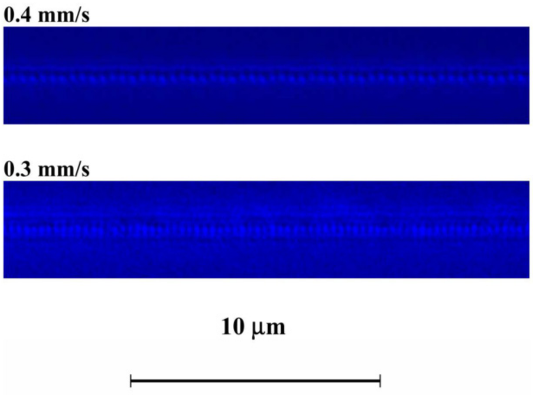

Figure 7. DIC microphotographs of structures with 400 and 300 nm periods inscribed at the optimal focus depth of 170 µm with sample translation speeds of 0.4 and 0.3 mm/s, respectively. The energy of the inscribing pulses was 90 nJ. The size of the bar corresponds to 10 µm.

the Plan-Apochromat x100 oil-immersed objective used for DIC measurements had its minimum of aberrations at the depth of 170 µm as well. We believe that the positioning of the inscribed periodic structure at the depth of the best resolution of the monitoring objective enabled us to detect the lowest period of inscription.

The minimal pulse energy value of 30 nJ used for the inscription can be compared with the typical pulse energy value of 600 nJ used earlier in 800 nm nanostructure fabrication [10, 11]. Such a decrease in the inscription energy is in line with the decrease of the order of the absorption process, from five-photon to two-photon [14, 17]. It should be emphasized that the laser pulse peak power values used in our experiments (100-300 kW) correspond to the critical power for self-focusing in fused silica, which at 267 nm is estimated to be ~250 kW (see below). The importance of the 170-µm-thick glass layer for the substantial decrease of the focal beam spot is undoubtedly related to nonlinear effects.

5. Numerical modeling

For numerical modeling of the plasma formation during nonlinear propagation of high-intensity femtosecond 267 nm laser pulse through fused silica media with subsequent two-photon absorption (TPA) and self-focusing, the adaptive mesh approach [20, 21] was used. This approach was already used earlier for the theoretical description of the five-photon absorption case, which takes place while the high-intensity 800 nm femtosecond pulse is propagating through the same medium [10, 11]. Here we will present only some essential results of numerical calculations for UV PbP inscription, the detailed description will be published elsewhere.

First we will determine some physical parameters for 267 nm case, which will allow the better understanding of the described effect. One of these parameters is the critical self-focusing power

$$P_{cr} = \frac{\lambda^2}{2\pi\, n\, n_2}, \qquad (1)$$

where λ is the inscription wavelength, n is the linear refractive index at the inscription wavelength [22] and n_2 is the nonlinear refractive index which is for fused silica nearly constant through the high transparency region and equal to $3{\times}10^{-16}$ cm^2/W [22]. The calculation made gives a value of about 250 kW. This is by an order of magnitude smaller than the similar value for 800 nm case (2300 kW [11, 20]).

The second important parameter is the I_{th}, "threshold intensity for femtosecond inscription to begin", which follows from the rate equation for plasma generation under femtosecond laser excitation [10, 11]:

$$I_{th} = \sqrt{\frac{2\, h\nu\, \rho_{BD}}{\tau_p\, \beta}}, \qquad (2)$$

where $h\nu$ is the photon energy at 267 nm, ρ_{BD} is the critical (breakdown) density of plasma ($\rho_{BD} \approx 1.6{\times}10^{22}$ 1/cm^3), τ_p is the femtosecond pulse duration, β is the two-photon absorption coefficient (for fused silica at the given irradiation wavelength $\beta = 2{\times}10^{-11}$ cm/W [23]). The calculations made give for the threshold of femtosecond inscription at 267 nm the value of about $6{\times}10^{13}$W/cm^2.

The upper limit for the intensity for UV femtosecond microfabrication may be obtained with the following expression for the saturation intensity of TPA-induced ionisation:

$$I_{TPA} = \sqrt{\frac{1}{\sigma_2 \tau}} = \sqrt{\frac{h\nu\, \rho_{at}}{\beta\, \tau}}, \qquad (3)$$

where σ_2 is the absorption cross-section of two-photon transition, $\tau = 1.7{\times}10^{-15}$ s is the electronic collision relaxation time, ρ_{at}= $2.1{\times}10^{22}$ atoms/cm^3 is the material concentration. The calculations give for this parameter at 267 nm irradiation a value of $7{\times}10^{14}$ W/cm^2, which is by the order of magnitude higher than the value obtained above with the formula (2).

According to results of our numerical simulation (with the laser peak power of about P_{cr}, so-called the sub-critical regime of femtosecond inscription [24]) we found that the pulse intensity never reaches I_{TPA} ($7{\times}10^{14}$ W/cm^2) regardless of the input laser pulse energy power and inscription depth. According to [24], the ratio of critical power for self-focusing and the threshold intensity for inscription defines a "critical" focal spot area:

$$S_{cr} = \frac{P_{cr}}{I_{th}}. \tag{4}$$

If the focal spot is larger than S_{cr} (linear focusing), the Kerr nonlinear term will contribute to the dynamics of focusing. The estimation using formula (4) gives for our case the value of the critical radius of around 360 nm. As it was mentioned above, in our experiment we expect the focal spot radius to be of about 250-300 nm, which is close to critical radius.

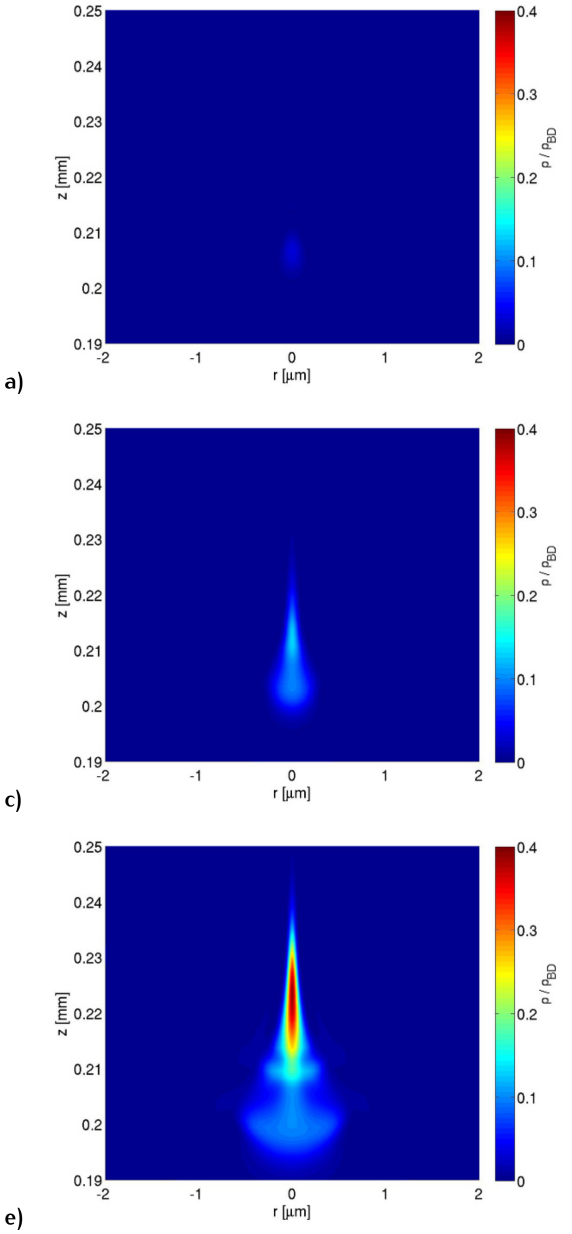

Figure 8. Plasma density distribution (normalized to plasma breakdown density) in a fused silica for the focusing depth of 200 µm and different laser radiation power values: (a) 0.2 P_{cr}; (b) 0.5 P_{cr}; (c) 1.0 P_{cr}; (d) 2.0 P_{cr}; (e) 5 P_{cr}. The vertical scale corresponds to the propagation direction (from down to up), while the horizontal scale corresponds to the transverse direction The colour scale designation corresponds to plasma density distribution normalized to plasma breakdown density.

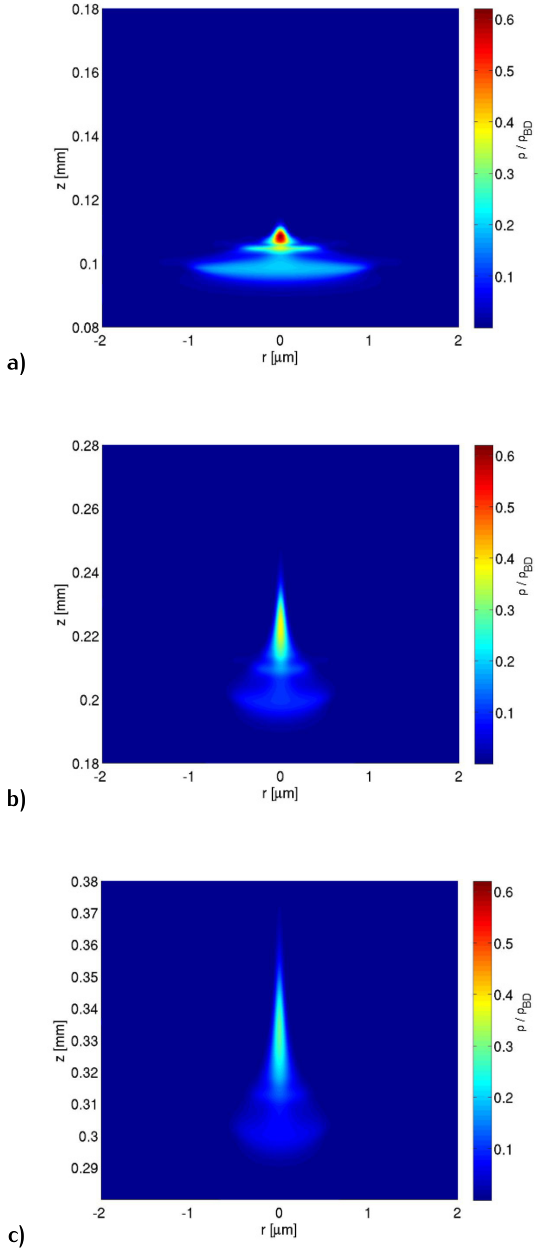

Figure 9. Plasma density distribution (normalized to plasma breakdown density) in a fused silica for laser radiation power of 5 P_{cr} and different focusing depths: (a) 100 µm; (b) 200 µm; (c) 300 µm. The vertical scale corresponds to the propagation direction (from down to up), while the horizontal scale corresponds to the transverse direction. The colour scale designation corresponds to plasma density distribution normalized to plasma breakdown density.

This means that we should expect the contribution of nonlinear effects. Using the formula (5) from [24], we could deduce the threshold energy value for UV femtosecond inscription of 5nJ for a Gaussian beam. The six-time difference between this value and the experimental one (30 nJ) could be related to the non-Gaussian profile of the intensity distribution due to the specific design of our focusing objective.

Figs. 8a, b, c, d, e demonstrate calculated plasma density distributions (normalized to plasma breakdown density) in fused silica for the focusing depth of 200 µm and five different values of laser radiation power, from 0.2 P_{cr} to 5 P_{cr}. It is clearly seen how, with the raise of intensity, the self-focusing takes place and the "light bullet" forms. Figs. 9a, b, c demonstrate the plasma density distributions for three different focusing depths (100, 200 and 300 µm) and radiation power of 5 P_{cr}. It is evident that the focusing depth of 200 µm is optimal, as it corresponds to the smallest beam cross-section value. Hence the results of numerical calculations are in good agreement with our experimental findings.

6. Conclusion

Using 30 nJ, 267 nm, 300 fs laser pulses, tightly-focussed at a depth of 170 µm below the surface of a fused silica sample, we have succeeded in recording nanostructures with periods from 1000 nm to 250 nm. To the best of our knowledge, the latter period has never been achieved before from this type of inscription process. The optimisation of the fused silica layer thickness led us also to the inscription of the nanostructures with an improved quality. The performed numerical modeling confirms the obtained experimental results.

The gratings with a period of 250-360 nm inscribed in a fibre core could be used as efficient reflectors for Yb-doped (generation range around 1060 nm) or even shorter wavelength fibre lasers (down to 740 nm).

Acknowledgements

This work was funded by EPSRC (Grant EP/D060990/1). David N. Nikogosyan wishes to thank the Leverhulme Trust for his Visiting Professorship Award (Ref. F002250G). Padraig Bolger and Anatoly V. Zayats acknowledge the support from the EC FP6 project PLASMOCOM.

References

[1] E. Wikszak, J. Burghoff, M. Will, S. Nolte, A. Tünnermann, T. Gabler, In: Conference on Lasers and Electro-Optics, 16-21 May 2004, San-Francisco,

USA, OSA Trends in Optics and Photonics, 96, CThM7 (2004)

[2] A. Martinez, M. Dubov, I. Khrushchev, I. Bennion, In: Conference on Lasers and Electro-Optics CLEO/IQEC 2004, 16-21 May 2004, San-Francisco, USA, OSA Trends in Optics and Photonics, 96, CMY6 (2004)

[3] A. Martinez, M. Dubov, I. Khrushchev, I. Bennion, Electron. Lett. 40, 1170 (2004)

[4] A. Martinez, I. Y. Khrushchev, I. Bennion, Electron. Lett. 41, 176 (2005)

[5] Y. Lai, A. Martinez, I. Khrushchev, I. Bennion, Opt. Lett. 31, 1672 (2006)

[6] A. Martinez, I. Khrushchev, I. Bennion, Opt. Lett. 31, 1603 (2006)

[7] G. D. Marshall, M. Ams, M. J. Withford, Opt. Lett. 31, 2690 (2006)

[8] A. Martinez, M. Dubov, I. Khrushchev, I. Bennion, IEEE Photonic. Tech. L. 18, 2266 (2006)

[9] N. Jovanovic, A. Fuerbach, G. D. Marshall, M. J. Withford, S. D. Jackson, Opt. Lett. 32, 1486 (2007)

[10] M. Dubov, V. Mezentsev, I. Bennion, In: Proceedings of NSTI Nanotechnology Conference Nanotech 2006, 7-11 May 2006, Boston, USA, 3, 229 (2006)

[11] V. Mezentsev et al., Proc. SPIE 6459, 64590B (2007)

[12] I. Bennion et al., In: Proceedings of OSA Topical Meeting on Bragg Gratings Photosensitivity and Poling in Glass Waveguides BGPP 2007, 2-6 Sep. 2007, Quebec, Canada, BWB6

[13] C. W. Smelser, S. J. Mihailov, D. Grobnic, Opt. Express 13, 5377 (2005)

[14] D. N. Nikogosyan, Meas. Sci. Technol. 18, R1 (2007)

[15] D.-L. Wang, C.-D. Li, L. Luo, H. Yang Q.-H. Gong, Chinese Phys. Lett. 18, 65 (2001)

[16] M. Dubov, V. Mezentsev, I. Bennion, D. N. Nikogosyan, Meas. Sci. Technol. 18, L15 (2007)

[17] V. Kudriasov, D. Majus, V. Sirutkaitis, S. A. Slattery, D. N. Nikogosyan, Opt. Commun. 271, 408 (2007)

[18] D. N. Nikogosyan, Nonlinear Optical Crystals: A Complete Survey (Springer, New York, 2005)

[19] R. Wiesendanger, Scanning Probe Microscopy (Springer, New York, 1998)

[20] V. Mezentsev, J. Petrovic, J. Dreher, R. Grauer, Proc. SPIE 6107, 61070R-1 (2006)

[21] J. S. Petrovic, V. Mezentsev, H. Schmitz, I. Bennion, Opt. Quant. Electron. 39, 939 (2007)

[22] D. N. Nikogosyan, Properties of Optical and Laser-Related Materials. A Handbook (John Wiley, Chichester, 1997)

[23] A. Dragomir, J. G. McInerney, D. N. Nikogosyan, Appl. Opt. 41, 4365 (2002)

[24] S. K. Turitsyn et al., Opt. Express 15, 14750 (2007)